Building and Environment 49 (2012) 310–323

Contents lists available at ScienceDirect

Building and Environment

journal homepage: www.elsevier.com/locate/buildenv

A heat transfer model for assessment of plant based roofing systems in summer conditions

Paulo Cesar Tabares-Velasco [1], Jelena Srebric*

Department of Architectural Engineering, The Pennsylvania State University, 222 Engineering Unit A, University Park, PA 16802-1417, United States

ARTICLE INFO

Article history:
Received 1 May 2011
Received in revised form
20 July 2011
Accepted 21 July 2011

Keywords:
Green roof
Heat and mass fluxes
Vegetated roof
Building energy
Evapotranspiration
Soil evaporation

ABSTRACT

This paper presents a quasi-steady state heat and mass transfer green roof model that can be incorporated in different energy simulation software or calculation procedures. The model considers heat and mass transfer processes between the sky, plants, and substrate. This paper also presents new equations to calculate (1) substrate thermal conductivity for green roofs, (2) substrate resistance to calculate green roof soil evaporation, (3) and set of compiled stomatal resistance functions to calculate plants' transpiration. The model is validated with robust experimental data that consists of surface temperatures, conduction heat flux, convection heat flux, net radiation and evapotranspiration. The data was obtained from laboratory experiments using a new "Cold Plate" apparatus set in an environmental chamber. The validation shows that the model predicts the heat and mass transfer accurately, except that it tends to underestimate peak evapotranspiration rates.

1. Introduction

Green roofs are specialized roofing systems that support vegetation growth on human-made structures such as rooftops [1,2]. Green roofs are classified as extensive and intensive green roofs. Extensive green roofs when compared to intensive green roofs have lower weight, lower capital cost, minimal maintenance, and a substrate depth between 5 cm and 15 cm [1,3]. Typical weight increase on the roof due to extensive green roof materials is from 72 kg/m^2 to 169 kg/m^2. In comparison, intensive green roofs have higher capital costs, wider planting selection, higher maintenance requirements, and increased substrate depth between 20 cm and 60 cm, which results in increased weight on the roof from 290 kg/m^2 to 968 kg/m^2 [1]. Thus, intensive green roofs cost more than extensive green roofs because they required additional structural support, require irrigation and have a deeper substrate layer [1,4]. Moreover, extensive green roofs are the most common green roof, representing about 2/3 of the total green roof area installed in North America [5]. Therefore, our modeling efforts focus on extensive green roofs as a more economically viable solution to be adopted in buildings.

From top to bottom, a typical green roof consists of several layers: (1) vegetation, (2) substrate, (3) filter membrane, (4) drainage layer, and (5) root resistance layer. Plants used on green roofs range from native plants and grasses to drought tolerant plants such as *Sedum* and *Delosperma* species, which belong to the cactus family of plants. Therefore, *Sedum* and *Delosperma* are hardy succulent plants, and have the ability to survive in drought conditions by limiting their water loss due to transpiration. Substrate is a lightweight porous soil-like layer that supports plant growth by retaining moisture and nutrients [3]. The substrate typically represents a mineral mix of sand, expanded clay, vermiculite, perlite, gravel, crushed brick, peat, organic matter and some soil [1]. The filter or cloth membrane prevents drainage clogging by containing the substrate and roots, and sometimes comes coupled with the drainage layer. The drainage layer transports the rainfall runoff to the roof drain, and ventilates/aerates the substrate and consists of large size gravel, expanded clay, lava and pumice stone or plastic/polystyrene webbing or chambers, resembling an egg carton shape. Finally, the root resistance layer prevents root penetration into the roof membrane [1,3,6].

Plants' architecture can be characterized by plants' height. A more relevant characteristic for thermal performance modeling is the leaf area index (LAI) [7]. Definition of LAI varies depending on the field of study or approach taken [8]. The most common

* Corresponding author. Present address: National Renewable Energy Laboratory, 1617 Cole Blvd. MS 5202, Golden, CO 80401, United States. Tel.: +1 303 384 7591; fax: +1 303 384 7495.
E-mail addresses: paulo.tabares@nrel.gov (P. C. Tabares-Velasco), jsrebric@engr.psu.edu (J. Srebric).
[1] Present address: National Renewable Energy Laboratory, 1617 Cole Blvd. MS 5202, Golden, CO 80401, United States. Tel.: +1 303 384 7591; fax: +1 303 384 7495.

0360-1323/$ – see front matter © 2011 Elsevier Ltd. All rights reserved.
doi:10.1016/j.buildenv.2011.07.019

definition of LAI is the projected or shadow leaf area divided by the ground area. However, other studies recommend the use of half of the total intercepted leaf area divided by the ground area as a more robust definition for all types of leaves [9].

Most of the water losses in plants (transpiration) are through plant stomata. Stomata are adjustable small pores in the leaf that allow the entry of gases needed for photosynthesis such as CO_2, and the release of O_2 and water vapor. Thus, this is a natural control mechanism that allows plants to control their transpiration rate by opening and closing their stomata [10–12]. Thus, when modeling green roofs, it is important to accurately understand the physiological behavior of typical plants used on green roofs.

Green roofs are regarded as a sustainable technology that potentially offers several benefits to society and the environment depending on the building design and location of the building. Among the most cited benefits are: (1) reduced building energy demand on space conditioning, (2) reduced storm water runoff, (3) expanded lifespan of roofing membranes, and (4) reduced urban heat island effect in cities. To understand the potential for reduced cooling energy demand, the thermal performance of green roofs has been investigated worldwide using three different approaches: (1) field or laboratory experimentation, (2) theoretical/numerical studies, and (3) a combination of laboratory or field experiments with numerical models. Field experimental studies have focused on measuring:

- heat flux reduction [2,13–18],
- green roof R-value [16] and/or
- evapotranspiration rates [19–22].

All of these field experimental studies measured these different green roof thermal performance parameters under unsteady weather conditions and using field instrumentation. In contrast, there are only few laboratory studies focused on quantifying the same thermal performance [23–28]. These laboratory studies tried to minimize stochastic weather forcing on heat transfer by controlling environmental conditions and to improve the accuracy of collected data by using laboratory-rated instrumentation. However, these studies did not measure all of the heat and mass transfer processes simultaneously, which is important for validation of model components, rather than just evaluating overall heat transfer rates. In addition, field or laboratory experimentation has the limitation of representing only a few different climates or building designs. These limitations can be overcome with a comprehensive and reliable heat and mass transfer model for green roofs.

Modeling the thermal performance of green roof is challenging due to the complex heat and mass transfer through the roof resulting from the shading, insulation, evapotranspiration, and thermal mass [29]. As a result, the modeling of green roofs is not an easy task because the thermal properties of a green roof depend on dynamic factors such as the plant growth, substrate thermal properties, and substrate water content. Based on an extensive literature review, the first modern theoretical green roof model was developed in India [30]. Since then, researchers have modeled green roofs by using steady state R-values [16,31,32] and accounted for plant materials by further adjusting the radiative/spectral properties [2,13,33], and/or by using equivalent albedo that combined a constant latent heat flux and/or photosynthesis rate [34,35].

More robust models have implemented energy and mass balance across the roof and calculated evapotranspiration rates. There are several models that use an energy balance modeling approach across green roofs [30,36–40]. The simpler versions of these models use the quasi-steady-state approach [38–40], which is similar to models for heat transfer on vegetated surfaces [41]. Other studies account for the thermal storage of the substrate [30,37]. In addition, a couple of models have simulated green roofs by coupling heat and mass transfer processes. A coupled heat and mass transfer model took into account water movement in the substrate, but it required knowledge of water content changes [22]. Looking also into the urban heat island effect, another study concluded that adding mass transfer into the analysis improved predictions of surrounding air temperatures [42]. A different model grouped convective and radiative heat transfer into an adduction coefficient and calculated evapotranspiration using the Penman equation. Thus, the model performed well when the roof was wet, but not in dry conditions, because the Penman equation does not contain a term to account for stomatal resistance [43]. Finally, a recent green roof model [44] presented an adaptation of Soil-Vegetation-Atmosphere Transfer (SVAT) schemes used in meso-scale meteorological analyses or general circulation models [45]. The parametric study of this model showed that increased soil thickness and LAI can result in building energy savings during winter and summer. However, high LAI values in winter are uncommon, as many plants are dormant, thus losing their leaves, which decreases LAI. Overall, previous green roof models have conducted heat and/or mass balance across green roofs to quantify thermal performance of green roofs. While different models agree that LAI plays an important role in reducing heat fluxes through a green roof, there is a disagreement about the role of substrate depth. Among the models that perform energy and/or mass balances, evapotranspiration is typically modeled with the Vapor Pressure Deficit (VPD) method [30,42,44,46]. As a result, most complete green roof models account for plant stomatal resistance and the resistance of substrate/soil to control water loss.

A complete green roof model should cover all of the relevant heat and mass transfer phenomena as well as their interactions. The main differences between models are: (1) factors affecting stomatal resistance, (2) convective heat transfer coefficient, and (3) substrate thermal conductivity. In order to understand these differences, it is necessary to experimentally quantify individual heat and mass transfer processes, so that modeling and laboratory work can address the remaining unanswered questions. In addition, some of these models were validated using only green roof surface temperatures obtained from field measurements. Nevertheless, a complete validation should also include heat transfer fluxes, such as heat flux through the green roof, convection, radiation, and evapotranspiration rates at the roof surface. An exhaustive literature review did not find a study that simultaneously measured all of the important heat and mass transfer processes in a green roof. Thus, the objective of this research study is to develop a model that is validated with a detailed heat and mass transfer data set from a new experimental apparatus "Cold Plate."

2. Green roof model

Previous research studies have shown that a green roof covered with plants has a different thermal performance from a green roof without plants [26,27]. A green roof has a different thermal performance from a bare substrate roof because of the plants' shading, transpiration, and wind shielding. However, it is also important to accurately model the performance of a green roof without plants because most of green roofs will not be 100% covered by plants through their lifespan. Thus, this study first considered a green roof without plants and then considered a green roof with plants. The green roof model without plants represents the worst case scenario when green roof is not yet established or all plants are dead. Therefore, this study presents both bear and fully-covered green roof models. Finally, these two models are combined in a model for partially-exposed/partially-covered green roofs,

which is perhaps the most realistic case for a real green roof in a building.

2.1. Green roof model without plants

The scenario of a roof covered with only green roof substrate represents the simplest way to simulate the roof for the worst case scenario when all plant material is not yet established or it dies. Energy balance across the green roof without plants is shown in Equation (1) for quasi-steady state environmental conditions:

$$R_n = Q_E + Q_{\text{sensible}} + Q_{\text{conduction}} \quad (1)$$

Equation (1) can be modified to have the heat losses to the surrounding air-sky grouped together in an overall film heat loss by means of convection, radiation, and evaporation, as following:

$$R_{sh,\text{abs}} = Q_{\text{film}} + Q_{\text{conduction}} \quad (2)$$

Fig. 1 shows a resistance thermal circuit that includes these individual heat transfer mechanisms.

In Equation (2), Q_{film} represents the heat transfer from the substrate to the environment by means of evaporation, convective heat transfer, and radiative heat transfer. Absorbed short-wave or solar radiation ($R_{\text{sh,abs}}$) is linearly proportional to the incoming short-wave radiation (R_{sh}) and is calculated using the following equation:

$$R_{sh,\text{abs}} = (1 - \rho_{\text{soil}})R_{sh} \quad (3)$$

Soil reflectivity (ρ_{soil}) depends on soil type and water content that typically varies from 0.10 for wet soil to 0.35 for dry soil. In contrast, soil emissivity ($\varepsilon_{\text{soil}}$) is not as dependant on water content, and typical values for soil emissivity are 0.90–0.98 [45]. Fig. 2 shows different albedo values measured for different soils and green roof substrates [45,47].

Overall, green roof model without plants includes equations for convection, evaporation, radiation, and conduction through the substrate.

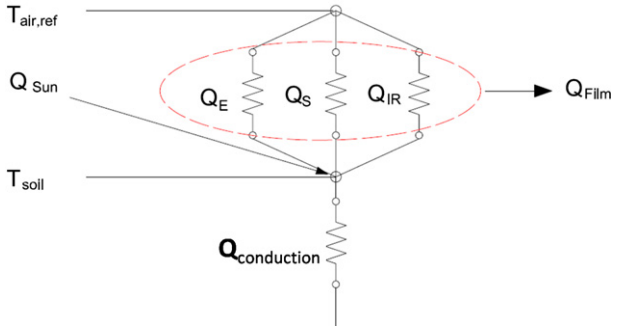

Fig. 1. Thermal circuit for heat fluxes considered in green roof model without plant material.

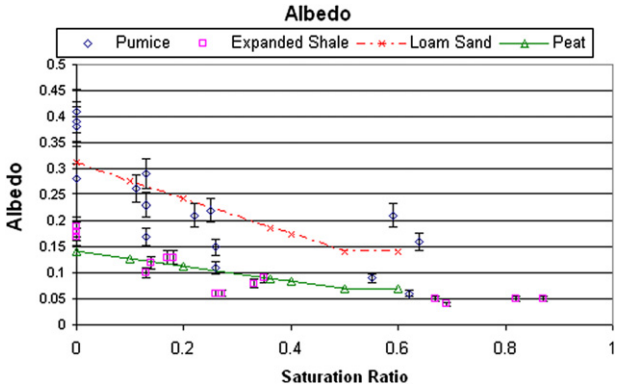

Fig. 2. Albedo for two soils (loam sand and peat) and two green roof substrates (pumice and expanded shale).

2.1.1. Convection heat transfer

The resistance to convective heat transfer is calculated using Equation (4). This equation calculates the Nusselt number for the forced, mixed, and natural convection on a flat surface depending on the ratio of the Grashof and Reynolds numbers [48]:

$$N_u = \begin{cases} 3 + 1.25 \times 0.025\text{Re}^{0.8} & Gr < 0.068\text{Re}^{2.2.} \quad \text{Forced Convection} \\ 2.7\left(\dfrac{Gr}{\text{Re}^{2.2}}\right)^{1/3}\left(3\dfrac{15}{4} + \dfrac{15}{16} \times 0.0253\text{Re}^{0.8}\right) & 0.068\text{Re}^{2.2.} < Gr < 55.3\text{Re}^{5/3} \quad \text{Mixed Convection} \\ 0.15Ra^{1/3} & 55.3\text{Re}^{5/3} < Gr \quad \text{Natural Convection} \end{cases} \quad (4)$$

2.1.2. Substrate evaporation

The second heat transfer mechanism in Fig. 1 is evaporative flux. Substrate evaporation is calculated using the following Equation (5):

$$Q_E = \frac{\rho C_p}{\gamma(r_{\text{substrate}} + r_a)}(e_{\text{soil}} - e_{\text{air}}) \quad (5)$$

where e_{air} is the vapor pressure in the air, e_{soil} is the saturated vapor pressure at the soil temperature, r_a is the aerodynamic resistance to mass transfer, and γ is the psychrometric constant, finally $r_{\text{substrate}}$ is the substrate surface resistance to mass transfer. This last resistance is based on the fact that as the soil surface dries, evaporation takes place at deeper soil levels, and thus the resistance to water vapor increases.

Here, the evaporation substrate resistance, $r_{\text{substrate}}$, was calibrated using a similar mathematical equation as the one used in previous soil evaporation models [49–52]. The calibration data for substrate evaporation rates were obtained in our previous experimental study [53] that is briefly described in Section 3.2. Substrate surface resistance to mass transfer was calculated by solving Equation (5) and by using: (1) the measured evaporation fluxes from the experiments without plants, (2) the vapor pressure in the air was calculated from "Cold plate" relative humidity and air temperature around the apparatus, (3) saturated vapor pressure of the soil was calculated from the substrate temperature measurements and (4) the aerodynamic resistance to mass transfer was calculated using equation (4) and assuming a Lewis number equal to 1. Additional explanation of these parameters and equations used can be found in the literature (11, 53).

The decision to develop a new set of coefficients for the substrate resistance to evaporation is based on the fact that the existing linear and nonlinear models, mostly power functions, for soil evaporation rates [49–51,54–57] were not consistent with the

experimental data [58]. It is important to note that the present study had laboratory-rated acquisition equipment, the "Cold Plate" apparatus, for detailed measurements of evapotranspiration rates by the gravimetric method, while simultaneously measuring the total energy balance on the green roof sample [53,58]. Therefore, this data set provides an opportunity to calibrate the evapotranspiration model specifically for extensive green roofs.

The proposed model used to calculate substrate resistance to evaporation is given in the following equation:

$$r_{\text{substrate}} = c_1 + c_2\left(\frac{\text{VWC}}{\text{VWC}_{\text{sat}}}\right)^{c_3} \quad (6)$$

where $c_1 = 0$ and $c_2 = 34.5$ and $c_3 = -3.3$ based on our experimental data set. Previously published values varied from 0 to 33 for c_1, from 3.5 to 270 for c_2, and from −1.6 to −2.3 for c_3 [49–52]. In Equation (6), VWC is the average substrate Volumetric Water Content (VWC) in the green roof substrate and VWC_{sat} is the substrate volumetric water content at saturation. It is important to mention that in the present study VWC is slightly different from VWC used to develop the previous soil models because the previous studies used only 0.5 cm–5 cm soil layer depth in contrast to the current study using 9 cm that represents a typical extensive green roof substrate depth. Equation (6) contains substrate volumetric water content based on previous suggestions that soil evaporation resistance models should include the amount of pores in the substrate, or the porosity [59,60]. For that reason, Equation (6) divides volumetric water content by the volumetric water content at saturation to account for the substrate porosity. A detail description of the volumetric water content profile, averaging procedure and comparison between previous models can also be found in the literature [58].

2.1.3. Long-wave radiative heat flux

The radiative heat flux between the sky and the substrate and its corresponding resistance to thermal radiative heat transfer for two bodies, one completely surrounding the other, are defined as following [61]:

$$Q_{IR} = \varepsilon_{\text{substrate}}\sigma\left(T^4_{\text{top, substrate}} - T^4_{\text{sky}}\right) \quad (7)$$

where $T_{\text{top,substrate}}$ is the upper substrate layer in contact with the air. There are many models to calculate the sky temperature. The simplest approach is to assume that the sky temperature is equal to the air temperature. Other simpler models assume that the sky temperature is the same to the air temperature minus 20 °C [62] or these models correlate downward long-wave radiation with the air temperature by adding empirical constants [38,63]. More complex models are not linear and depend on dew point temperature and time [61]. In this study, the sky temperature was obtained from the long-wave radiation measured from the pyrgeometer in the laboratory experiments assuming the room walls and lamps behave like a black body [53].

2.1.4. Conductive heat flux

The conductive heat transfer through the green roof substrate is calculated by Equation (8), where the thermal conductivity of the substrate is calculated using linear function with calibrated coefficients obtained from data collected with the "Cold Plate" apparatus [53]:

$$Q_{\text{conduction}} = k_{\text{substrate}}\frac{T_{\text{top, substrate}} - T_{\text{bottom, substrate}}}{L} \quad (8)$$

A linear equation agrees with a previous empirical model developed for a green roof substrate with similar density [64]:

$$k_{\text{substrate}} = a_1 + a_2 \times \text{vwc} \quad (9)$$

The values for a_1 and a_2 vary depend on a substrate type. For example: $a_1 = 0.16$ and $a_2 = 0.51$ for a substrate based on expanded clay [53]. An on-site study found $a_1 = 0.24$ and $a_2 = 0.30$ for a similar green roof substrate [64]. Moreover, in a third study, the values obtained are $a_1 = 0.17$ and $a_2 = 1.1$ for substrates based on pumice and $a_1 = 0.2$ and $a_2 = 1.4$ for substrate based on expanded shale [47].

2.2. Green roof model with plants

The green roof model with plants is different from the bare substrate roof model because it includes plants' shading, transpiration, and wind shielding. This model is an extension of the model for green roof without plants, and therefore the new thermal circuit incorporates these plant-related heat transfer phenomena as shown in Fig. 3.

Based on Fig. 3, and assuming negligible thermal storage and metabolic rate, the energy balance for the plant canopy and for the substrate underneath the plants is given by the following two equations, respectively:

$$R_{sh,\text{abs,plants}} = Q_{\text{film, plants}} + Q_{IR,S,P} \quad (10)$$

$$R_{sh,\text{abs,substrate}} = -Q_{IR,S,P} + Q_{s,s} + Q_{\text{conduction}} + Q_{IR,\text{subs, cov, sky}} + Q_E \quad (11)$$

where $R_{sh,\text{abs,plants}}$ is the absorbed short-wave radiation by the plants, and $Q_{\text{film,plants}}$ represents the heat transfer between plants and the surrounding environment by means of latent (transpiration), convective, and radiative heat transfer. In Equation (11), $R_{sh,\text{abs,substrate}}$ is the absorbed solar radiation by substrate underneath the plants, $Q_{IR,S,P}$ is the radiative or long-wave radiative heat transfer between the plant layer and the top substrate layer, $Q_{S,S}$ is the convective heat transfer between the top substrate layer and the surrounding air, $Q_{\text{conduction}}$ is the conductive heat flux through green roof substrate, and $Q_{IR,\text{subs,cov,sky}}$ is the thermal radiation exchanged between substrate and sky.

2.2.1. Absorbed short- and long-wave radiation

The amount of solar radiation absorbed by the plants ($R_{sh,\text{abs,plants}}$) and substrate underneath the plants ($R_{sh,\text{abs,substrate}}$) depends on the spectral properties of both surfaces, as well as the vegetation density in terms of LAI. Absorbed solar radiation by the plants is

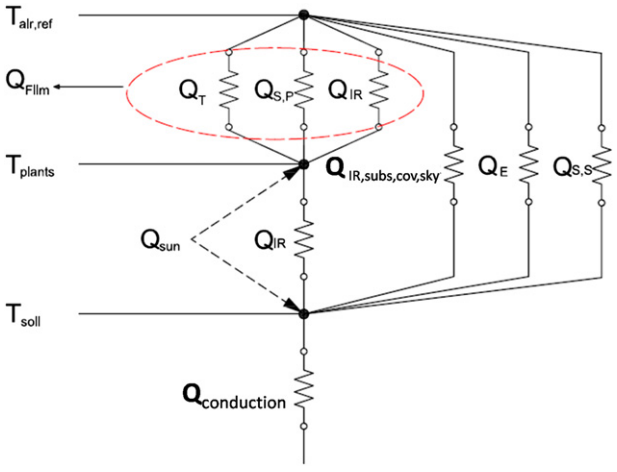

Fig. 3. Thermal circuit for heat fluxes considered in green roof model that includes plant material.

calculated using Equation 12 is similar to previous green roof studies [42,46]:

$$R_{sh,\mathrm{abs,plants}} = \left(1-\rho_{\mathrm{plants}}-\tau_{\mathrm{plants,solar}}\right)\left(1+\tau_{\mathrm{plants}}\,\rho_{\mathrm{substrate}}\right)R_{sh} \quad (12)$$

where $\tau_{\mathrm{plants,solar}}$ is short-wave transmittance of a canopy ($\tau_{\mathrm{plants,\,solar}} = e^{-k_s \mathrm{LAI}}$), and k_s is the extinction coefficient.

In Equation (12), the amount of intercepted solar radiation depends on the transmittance of the plant layer, which in turn depends on the solar altitude and leaf orientation as reviewed in Table 1 and Table 2. For horizontal flat leaves, the transmittance remains constant.

Furthermore, the absorbed solar radiation for the substrate underneath the plants ($R_{sh,\mathrm{abs,substrate}}$) represents the amount of radiation that is not intercepted by the leaves, transmitted ($\tau_{\mathrm{plants,solar}}$) or reflected ($\rho_{\mathrm{substrate}}$) to the substrate. In this study, the absorbed solar radiation is calculated using the following equation:

$$R_{sh,\mathrm{abs,substrate}} = \tau_{\mathrm{plants,solar}}(1-\rho_{\mathrm{substrate}})R_{sh} \quad (13)$$

In addition to the solar radiation, the thermal radiation between sky, plants, and green roof substrate can play an important role, especially when the sky is clear. This model calculates, thermal radiation using the following two equations:

$$Q_{IR,\mathrm{plants,\,sky}} = \left(1-\tau_{\mathrm{plants},IR}\right)\varepsilon_{\mathrm{plants}}\sigma\left(T^4_{\mathrm{plants}}-T^4_{\mathrm{sky}}\right) \quad (14)$$

$$Q_{IR,\mathrm{substrate,cov,sky}} = \left(\tau_{\mathrm{plants},IR}\right)\varepsilon_{\mathrm{substrate}}\sigma\left(T^4_{\mathrm{plants}}-T^4_{\mathrm{sky}}\right) \quad (15)$$

The transmittance of thermal radiation $\tau_{\mathrm{plants},IR} = e^{-k_1 LAI}$, stands for the radiation that will not be intercepted by any leaf. $\tau_{\mathrm{plants},IR}$ is calculated with the same equation as $\tau_{\mathrm{plants,solar}}$ by using a different extinction coefficient as shown in Table 1 and Table 2. In Equation 14 and 15, $\varepsilon_{\mathrm{plants}}$ represents plant emissivity and $\varepsilon_{\mathrm{substrate}}$ represents substrate emissivity. Substrate emissivity is about 0.95 [63]. The emissivity for leaves ($\varepsilon_{\mathrm{plants}}$) is reported in the literature as 0.96, but it can be as low as 0.92 and as high as 0.98 [10,66]. For example, grass emissivity ranges from 0.90 to 0.97 [45], while cactus emissivity is 0.98 [63].

Overall, for most common plant leaves, the total solar absorptance is from 0.4 to 0.6, typically used as 0.5 in calculations [10], having a solar transmittance of 0.20 and a solar reflectivity (ρ_{plants}) around 0.30 [7]. However, for desert succulent plants the solar absorptance is from 0.59 to 0.83, having a transmittance of zero [65]. Moreover, vegetated canopies tend to have lower reflectivity, from 0.15 to 0.24, due to multiple reflections and radiation trapping [62,63]. For example, short grass can have an albedo of 0.26, while 1 m long grass has an albedo of 0.16 [45]. A spectral reflectivity analysis for a green roof sample found a total measured solar reflectivity for a green roof sample around 0.06, a value below the reported values for grass or other plants [53]. The difference between the measured reflectivity and the value from the literature is because the reported reflectivity values in the literature are for leaves, while the value measured here combines the reflectivity of a vegetated canopy and underlying substrate [67].

Table 1
Canopy transmittance τ_d values for diffuse radiation [7].

LAI	Horizontal	Vertical	Uniform	Maize	Cotton
1	0.368	0.504	0.443	0.429	0.404
2	0.135	0.314	0.219	0.201	0.173
3	0.050	0.213	0.113	0.098	0.075

Table 2
The extinction coefficient k_s values for direct solar radiation [46,62,63].

Leaf Angle Distribution	Extinction Coefficient Equation for Direct Solar Radiation	Values			
		Direct Radiation			Long-wave Radiation
		Solar Elevation $\beta = 90°$	Solar Elevation $\beta = 60°$	Real Plants	
Horizontal	1	1	1	Clover: 1.1 Sunflower: 0.97	1–1.05
Cylindrical (Vertical) $\alpha = 90°$	$2/\pi \cdot \tan(\beta)$	0.00	0.37	Ryegrass: 0.43–0.29	0.436
Spherical	$1/2 \cdot \sin(\beta)$	0.50	0.58	N/A	0.684–0.81
Conical $\alpha = 60°$	$\cos(\alpha)$	0.50	0.50	N/A	0.829
$\beta > \alpha$[a] $\alpha = 30°$		0.87	0.87	N/A	($\alpha = 45°$)

[a] Cone wall angle.

2.2.1.1. Long-wave radiation between plants and substrate. Radiation exchange between the plant canopy and the top layer of substrate is very complex and difficult to calculate. However, several assumptions can be made to simplify the calculations. The most common assumption used in green roof modeling, borrowed from the meteorological mesoscale models, is to represent plants and substrate as two flat plates/surfaces. This assumption is not necessarily valid for large trees, but it is fairly realistic for low stature plants, which tremendously simplifies the calculation. Overall, the radiative heat exchange can be calculated using the following three assumptions [61]:

1. Two parallel surfaces with different areas,
2. Two infinite parallel plates/surfaces, and
3. Small area (substrate) surrounded by a large enclosure (plants).

Most of the green roof models have used assumption 3 [42,46] or assumption 2 [44]. However, assumption 1 represents conditions that are most realistic, as the total surface area of the leaves is higher than the substrate surfaces for higher LAI. Thus, this study initially applied assumption 1 in Equation (16):

$$Q_{IR,S,P} = (1-\tau_{IR})\,\frac{\sigma\left(T^4_{\mathrm{plants}}-T^4_{\mathrm{top,\,substrate}}\right)}{\dfrac{1-\varepsilon_{\mathrm{substrate}}}{\varepsilon_{\mathrm{substrate}}}+\dfrac{1-\varepsilon_{\mathrm{plants}}}{\varepsilon_{\mathrm{plants}}\cdot \mathrm{LAI}}+\dfrac{1}{F_{\mathrm{view}}}} \quad (16)$$

From the three approaches, assumption 1 requires the most information, as one must determine the view factor that depends on LAI as well as plant height [68]. To select a model for thermal radiation, the three modes were tested using LAI and surface temperature values from the "Cold Plate" apparatus. The results from the three approaches differed less than 10%, or less than 4 W/m^2. The reason for similar values between the three approaches is probably due to the similar emissivity values of the substrate and plants, which are close to 1. From the three assumptions, the model with assumption 1 consistently obtained the lowest value, followed by the model with assumption 2. As a result, this study will use assumption 2 because the added simplicity does not compromise the accuracy of the calculations:

$$Q_{IR,S,P} = (1-\tau_{IR})\,\frac{\sigma\left(T^4_{\mathrm{plants}}-T^4_{\mathrm{top,substrate}}\right)}{\dfrac{1}{\varepsilon_{\mathrm{substrate}}}+\dfrac{1}{\varepsilon_{\mathrm{plants}}}-1} \quad (17)$$

2.2.2. Convective heat transfer

The convective heat transfer coefficient is calculated using Equation (4), originally developed for horizontal flat plates. Thus, this

study has added a coefficient to account for the roughness of the plants. The coefficient is based on previous research for convective heat transfer of plant leaves [69]. In addition, convective heat transfer at the substrate is calculated using an equation developed for convection of porous media [70], assuming the air speed in the porous media is 1/3 of the air speed above the plants [71]:

$$Q_{\text{convection, plants}} = 1.5 \cdot \text{LAI} \cdot h_{\text{conv}} \left(T_{\text{plants}} - T_{\text{air}} \right) \quad (18)$$

$$Q_{\text{convection,substrate,cov}} = h_{\text{sub}} \left(T_{\text{substrate,top}} - T_{\text{air}} \right) \quad (19)$$

The substrate convective heat transfer coefficient, $h_{\text{sub}} = h_{\text{por}} \cdot h_{\text{conv}} / (h_{\text{por}} + h_{\text{conv}})$, is based on the Nusselt number for porous media, $Nu_{\text{por}} = 1.128 Pe^{0.5}$ [69], which is based on the Péclet number, $Pe = 0.3\, V_{\text{air}} \text{Length} / \alpha_{\text{por}}$ [70,71]. The thermal conductivity of the porous media, in this case the plant layer $k_{\text{por}} = \phi \cdot k_{\text{air}} + (1 - \phi) k_{\text{plants}}$, depends on the porosity of the plant layer (ϕ) and the thermal conductivity of air, k_{air} [70]. The leaf thermal conductivity, k_{plants}, varies from 0.27 to 0.57 W/m K [72]. Because typical extensive green roof plants are succulent plants with high leaf water content, the thermal conductivity is selected to be 0.50 W/m K. Porosity equal to 0.85 was selected based on plant height and LAI measurements [53].

2.2.3. Evapotranspiration

A particularly important heat fluxes shown in the energy balances in Equation (10) and Equation (11) are substrate evaporation and plant transpiration, especially when considering reduction of cooling loads in buildings. Substrate evaporation is calculated using Equation (5) and Equation (6), while modeling the plants as porous media. Furthermore, plant transpiration is calculated using Equation (20). The stomatal resistance, r_s, is calculated using the multiplicative approach shown in Equation (21), originally proposed by Jarvis [73]. Similar versions of Equation (21) have been adopted by most recent green roof and SVAT models:

$$Q_T = \text{LAI} \frac{\rho C_p}{\gamma (r_s + r_a)} \left(e_{s,\text{plants}} - e_{\text{air}} \right) \quad (20)$$

$$r_s = \frac{r_{\text{stomatal,min}}}{\text{LAI}} \cdot f_{\text{solar}} \cdot f_{\text{VPD}} \cdot f_{\text{vwc}} \cdot f_{\text{temperature}} \quad (21)$$

Each of the empirical functions "f" in Equation (21) represents a role that different environmental and plant variables, such as solar radiation (f_{solar}), vapor pressure deficit (f_{VPD}), water content (f_{VWC}), and temperature ($f_{\text{temperature}}$), play in stomatal resistance/aperture and, consequently, in plant transpiration. Our study collected different expressions of these functions from several published SVAT or green roof models [45,71,73–82]. These functions were developed in different environmental conditions and for different plant types, such as tropical trees or desert shrubs. Thus, they predict different stomatal resistance for similar environmental conditions. Interestingly, no previous study has evaluated whether these functions are valid in a green roof sample. Our study evaluated and compared the functions with experimental data collected for *Sedum spurium* and *Delosperma nubigenum*, two typically used green roof plants [3]. The goal was to assess the impact that solar radiation, substrate water content, vapor pressure deficit (VPD), and temperature have on plant transpiration. The total number of functions evaluated is [58]:

1. 9 functions for solar radiation,
2. 8 functions for water content,
3. 6 functions for VPD, and
4. 2 functions for temperature.

12 quasi-state steady green roof data sets from the "Cold Plate" were used (6 with low air speed and 6 with high air speed). From the data set, the minimum stomatal resistance was found to be around 500–700 s/m. This value is within the expected range of 450–1000 s/m for succulent plants and 225–1125 s/m for desert plants [62]. The models that performed the best are presented in Fig. 4. Models shown in Fig. 4 are:

- D-1: Combination of empirical functions (f_{solar}, f_{VWC}, f_{VPD}, $f_{\text{temperature}}$) from the following studies respectively [77,80,83,84]
- D-2: Similar to D-1 but empirical function f_{VWC} was modified from [84]
- D-3: Similar to D-1 but empirical function f_{VWC} was modified from [83,84]
- D-4:Combination of empirical functions (f_{solar}, f_{VWC}) proposed by another green roof model [44]
- D-5: Combination of empirical functions (f_{solar}, f_{VWC}, f_{VPD}, $f_{\text{temperature}}$) proposed by a mesoscale model [77]
- D-6: Combination of empirical functions (f_{solar}, f_{VWC}, f_{VPD}, $f_{\text{temperature}}$) from the following studies respectively [73,82–84]

The continuous line in Fig. 4 represents perfect agreement between measured data and resistances calculated by different models. The best agreement is obtained for a D-3 model that incorporates a sub-component for VPD that was empirically developed for desert plants. There is another stomatal model, D-6, which provided similar results as the selected model D-3. However, D-3 model was selected because D-6 tends to overestimate minimum stomatal resistances. Overall, D-3 model performs well, but it tends to overestimate stomatal resistance when the substrate has high volumetric water content.

The functions selected to calculate stomatal resistance were developed from different studies: f_{solar} was based on tobacco plant measurements [77], f_{VWC} is a modified version of previous model [78], f_{VPD} follows the logarithmic approach used for desert plants [80,81], and $f_{\text{temperature}}$ is not subject to a large debate in the literature and it follows the same form as in SVAT models [60,74,84]. The complete set of proposed functions for the developed stomatal resistance model is shown in Equation (22) to Equation (25):

$$f_{\text{solar}} = 1 + e^{-0.034(R_{sh} - 3.5)} \quad (22)$$

$$f_{\text{VWC}} = \begin{cases} 1 & \text{VWC} > 0.7\text{VWC}_{fc} \\ \dfrac{0.70\text{VWC}_{fc} - \text{VWC}_{wp}}{\text{VWC} - \text{VWC}_{wp}} & \text{VWC}_{wp} < \text{VWC} < 0.7\text{VWC}_{fc} \\ 1000 & \text{VWC}_{wp} > \text{VWC} \end{cases} \quad (23)$$

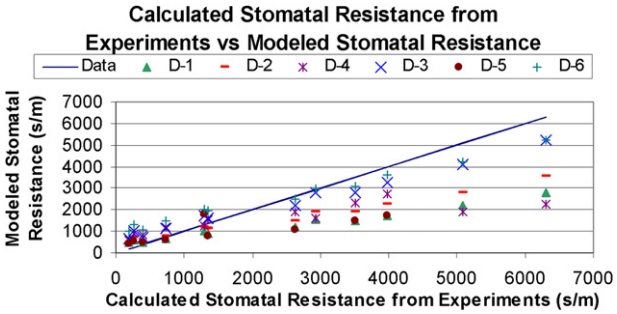

Fig. 4. Comparison of stomatal resistance for six different models based on Equation 20 and a set of measured data in "Cold Plate" apparatus for *Sedum spurium* and *Delosperma nubigenum*.

$$f_{\mathrm{VPD}} = \frac{1}{1 - 0.41\ln\left(e_{s,\mathrm{plants}} - e_a\right)} \tag{24}$$

$$f_{\mathrm{temperature}} = \frac{1}{1 - 0.0016\left(35 - \left(T_{\mathrm{plants}} - 273.15\right)\right)^2} \tag{25}$$

The value of 30 °C in Equation (25) is slightly higher than the originally proposed one in the literature [78]. This temperature value corresponds to the leaf temperature with a maximal stomatal opening. This temperature value ranges from 20 to 35 °C, but typically is around 30 °C [85].

In real applications, energy modelers might encounter green roofs with different plants. As explained in the Introduction, this research focus on extensive green roof systems that typically use low statue plans such as succulent and desert plants. Thus, the values found in this research and the expected range referenced here could guide energy modelers to make more educated guesses about the stomatal resistance.

2.3. Green roof partially covered with plants

Most of the green roof models have assumed that the plants are healthy and fully covering the roof. However, this assumption may be far from reality. Thus, a robust green roof model should also consider the plant coverage (σ_f) of the green roof. Assuming a parallel circuit between a roof covered by plants and a bare substrate roof, the heat transfer through the roof and the total evapotranspiration can be calculated as following:

$$Q_{\mathrm{substrate}} = \sigma_f Q_{\mathrm{substrate,\ covered}} + \left(1 - \sigma_f\right) Q_{\mathrm{substrate,\ bare}} \tag{26}$$

$$Q_{ET,\ \mathrm{total}} = \sigma_f \left(Q_{E,\mathrm{substrate,\ cov}} + Q_{T,\mathrm{plants}}\right) + \left(1 - \sigma_f\right) Q_{E,\mathrm{substrate,bare}} \tag{27}$$

In conclusion, for a green roof that is only partially covered, the model for a green roof with plants and without plants should be evaluated simultaneously to calculate the total heat flux through the roof.

3. Verification and validation

After the model is developed, the next step is verification and validation. Verification and validation are procedures to assess whether a model is correctly simulating the actual physical phenomena of a system. A new apparatus was developed to obtain required heat and mass transfer fluxes for a complete verification and validation [53,58].

3.1. "Cold Plate" apparatus description

Based on literature, a new experimental apparatus was needed to address shortcomings in the existing data sets on energy balance for green roofs. The new apparatus, named "Cold Plate," was designed to include laboratory-rated instrumentation and to allow simultaneous measurements of all important heat and mass transfer processes on a green roof. The "Cold Plate" apparatus is located inside a full-scale environmental chamber. This apparatus enabled experiments isolated from stochastic outdoor conditions. The controlled environmental conditions included airflow rate, temperature, and humidity, which represent quasi-steady state air parameters in outdoor environment. The design and construction of experimental apparatus for testing green roof thermal properties was a challenging process that included several versions of the apparatus. The final version of the apparatus uses laboratory-rated instrumentation to measure the next variables of interest and as shown in Fig. 5. A more detailed explanation of the apparatus, environmental parameters simulated inside the environmental chamber, and a more extensive description of experimental results can be found in the literature [27,53]:

1. Evapotranspiration –Measured by continuously keeping track of changes in: (1) weight using a high-resolution scale or platform and (2) in volumetric water content in the substrate using a water content reflectometer.
2. Incident incoming short-wave radiation – Measured with a secondary class pyranometer.
3. Incident incoming long-wave radiation – Measured by a laboratory-rated pyrgeometer.
4. Outgoing long-wave radiation– Calculated using measured average plant and top substrate surface temperatures.
5. Heat fluxes through the green roofs – Measured by installing heat flux meters underneath the green roof and also by making energy balance around the "Cold Plate."
6. Convective heat transfer fluxes – Indirectly measured by subtracting all measured heat flows in the total energy balance Equation (1) or combination of Equations (10) and (11).
7. Substrate top and bottom layer temperatures – Measured with waterproof thermistors. The thermistors in the substrate top were located just under a thin layer of substrate to measure the top substrate temperature. The thermistors at the bottom of the substrate layer were located between the lower part of the substrate and the filter cloth membrane.
8. Substrate thermal conductivity – Calculated from the quasi-steady state measurements of: (1) heat flux through the substrate, (2) temperatures at the top substrate and (3) temperature at the bottom substrate layer.
9. Plant temperatures – Measured by thermistors attached to plant leaves. Additional infrared pictures were taken during the last day of experiments to corroborate the measured surface temperature.
10. Average substrate volumetric water contents – Measured by diagonally inserted water content reflectometers.
11. Air velocities – Measured with omnidirectional hot-sphere anemometers that were located at different locations around the green roof samples to obtain a good velocity profile.
12. Room air relative humidity levels and temperatures – Measured with relative humidity and temperature sensors located in the environmental chamber return ductwork.
13. Spectral reflectivity of green roof samples – This measurement was the only variable measure outside of the Cold Plate apparatus as it required more space and very sensitive equipment.

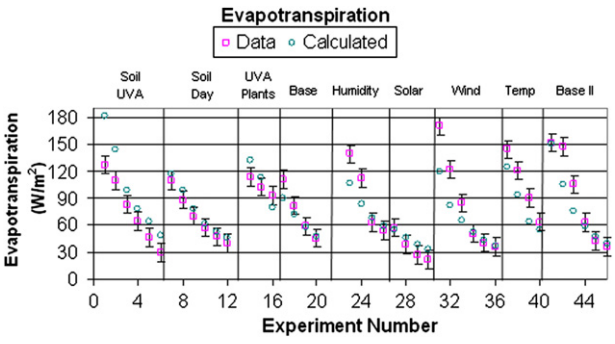

Fig. 5. Measured (squares) and calculated (circles) evapotranspiration fluxes.

The combine reflectivity of the plants substrate was measured with a Portable Spectroradiometer using a calibrated lamp different that the fluorescent lamps directly above plants.

14. Leaf Area Index (LAI) – Measured manually by leaf count and measuring several leaf dimensions in several grid points for sample with *D. nubigenum*.

Overall, more than 9 experiments where conducted in a one year period, following a 3 year design/build process that involved different environmental conditions, two green roof samples with *S. spurium* and *D. nubigenum*, one sample without plants as explained bellow [53,58]:

1. Soil UVA. Solar radiation simulated with UVA lamps for the experiment with a green roof sample without plants. Test lasted 6 days
2. Soil Day. Solar radiation simulated with Fluorescent Daylighting VHO lamps for the experiment with green roof sample without plants. Conditions equal to San Francisco cooling design conditions [86]. Test lasted 6 days
3. UVA Plants. Solar radiation simulated with UVA lamps for the experiment with a green roof sample with *S. spurium*. Test lasted 3 days
4. Base. Solar radiation simulated with Fluorescent Daylighting VHO lamps for the experiment with green roof sample with *Delosperma nubigenum*. Conditions equal to 'Soil Day' experiment. Test lasted 4 days.
5. Humidity. Conditions equal to 'Base' experiment, except that relative humidity was set to 50%. Test lasted 4 days.
6. Solar. Conditions equal to 'Base' experiment, except that solar radiation decreased by 50%. Test lasted 4 days.
7. Wind. Conditions equal to 'Base' experiment, except that wind speed increased to 1 m/s. Test lasted 6 days.
8. Temp. Conditions equal to 'Base' experiment, except the air temperature changed to 26 °C. Test lasted 2 days.
9. Temp. Conditions equal to 'Base' experiment, except air temperature changed to 24 °C. Test lasted 2 days.
10. Base II. Conditions equal to 'Base' experiment. Test lasted 6 days

The UVA lamps were initially used because they provide higher irradiance. However, the amount of UVA radiation was higher than what is naturally available outdoor thus plants started to wilt after a single 3-day test. Therefore, the rest of the experiments with plants used Daylight Fluorescent lamps (VHO). Although not the same as natural daylight, these lamps have an almost constant wavelength output in the visible range compared to the other fluorescent lamps that have a higher output in the yellow-orange-red part of the spectrum. Therefore these lamps produce light as close as possible to solar radiation. This is important, as plants behave differently to the visible and the infrared part of the spectrum: have reflectivity that depends on the wavelength and their stomatal response is mainly sensitive to visible light.

3.2. Verification of individual heat transfer processes

The definition of verification procedure varies according to the area of research subject [86–88]. In this research project, verification would be understood as a process to evaluate the ability of the model components to simulate a specific physical phenomenon. Therefore, this paper presents a performance evaluation of specific model components with available experimental data. The objective of this verification process is to understand the capabilities of each of these three model components to predict the heat and mass transfer interactions between plants and the surrounding environment. Three fluxes were analyzed separately and the results are extensively described in the literature [58]. Table 3 summarizes the verified performance of the model components.

3.3. Laboratory steady state validation

The validation process builds on the previous knowledge about the model limitations discovered in the verification process. Therefore, in this paper, the validation is a procedure to demonstrate that the model can accurately predict green roof thermal performance. The validation process uses all of the experimental data collected in the "Cold Plate" apparatus under quasi-steady state conditions in the environmental chamber. The inputs required for validation are:

- air temperature,
- air relative humidity,
- air speed,
- sky temperature,
- incoming solar radiation,
- substrate water content,
- LAI, and
- bottom substrate temperature (boundary condition).

The bottom surface substrate temperature is the boundary condition used as an input in the current version of the green roof model. The sky temperature was calculated from the incoming long-wave radiation measured by a pyrgeometer [58]. The sky temperature value accounted for the surrounding air and lamps temperatures. Once all the data are inputted in the model, the variables to analyze are: (1) evapotranspiration, (2) convection, (3) conduction, (4) substrate temperature, (5) plant surface temperature, and (6) net radiation.

In addition, radiation from the fluorescent lamps was assumed to be diffuse and not direct. Thus, the sample with *Delosperma* is assumed to have a conical leaf angle distribution (see Table 2). The sample with *Sedum* is assumed to have a horizontal leaf angle distribution (see Table 2). Overall, the calculated canopy transmittance values τ_d for diffuse radiation are 20% lower for the samples with plants than for the samples without plants, which agrees with the data from another study shown in Table 1.

3.3.1. Evapotranspiration

Fig. 5 shows measured (squares) and calculated (circles) evapotranspiration fluxes. The graph is divided in 9 parts to indicate different experimental conditions as explained in Section 3.1. For example, "Soil UVA" has 6 square points that represent the measured values for the experiments without plants and using UVA lamps. In the same way, "Base" represents experiment 1 or the baseline benchmark. Additionally, the x-axis represents counter of all the experimental days involved. Data from experiments without plants only represent substrate evaporation because these two tests did not have any plant material. Overall, the model without plants works well, except during the first couple of days when it over predicts evaporation fluxes. Furthermore, the model with plants

Table 3
Root mean square error (RMSE) of model components obtained in the verification process.

Model Components	Green Roof Experiments without Plants	Green Roof Experiments with Plants
Evapotranspiration (W/m^2)	21	23.3
Convection (W/m^2)	23.6	26.3
Conduction (W/m^2)	2.1	4.3

also works well. The model follows the same trend as the experimental data, but it underestimates evapotranspiration when samples are the wettest, which is a consequence of the overestimated stomatal resistance. Fig. 5 shows similar results as in the verification process, which is a good result because it means that the plant and substrate temperature are well predicted.

3.3.2. Convective heat flux

Fig. 6 shows measured (squares) and calculated (circles) convective fluxes. As discussed in previous chapters, evapotranspiration and convection are strongly inter-related. Thus, the performance of the model shown in Fig. 6 is similar to the one observed in the verification process.

3.3.3. Heat flux through green roof substrate

Fig. 7 shows measured (squares) and calculated (circles) conduction heat fluxes. The model predicts lower heat flux reduction for the green roof samples with plants than with the green roof sample without plants. However, the model tends to overestimate heat fluxes in some cases. The case with higher air speed shows that the model output follows a different trend than the trend observed with experimental data. These discrepancies are due to thermal conductivity regression that worked well for most of the cases except for the case with higher wind, due to a lower temperature difference across the green roof sample [53]. Moreover, this result is probably due to the model underestimation of evapotranspiration during the first two days, the same time when the model overestimates heat fluxes though the substrate. The same problem occurs with the experiments using higher humidity levels. Thus, this proves how important is to estimate each of the different heat and mass transfer processes. Finally, the heat flux through the roof is directly proportional to the temperature difference between the top and bottom of the substrate. Therefore, these two temperatures will be analyzed in more details.

3.3.3.1. Substrate surface temperature. Fig. 8 shows measured (squares) and calculated (circles) substrate surface temperatures. Data from the experiments without plants represent the bare substrate temperature. In contrast, the data from the experiments with plants represents the temperature of the substrate covered by the plants. The model predicts the shading of the plants, but tends to overestimate the temperature of the substrate underneath the plants. The reason for the over prediction of substrate temperature could potentially be due to under prediction of the shading or soil evaporation. Another reason could be the albedo of the substrate, because no spectral reflectivity test was performed for the sample without plants. However, substrate also interacts with the plants by radiative heat transfer. Thus, the plants surface temperature will be analyzed in more details.

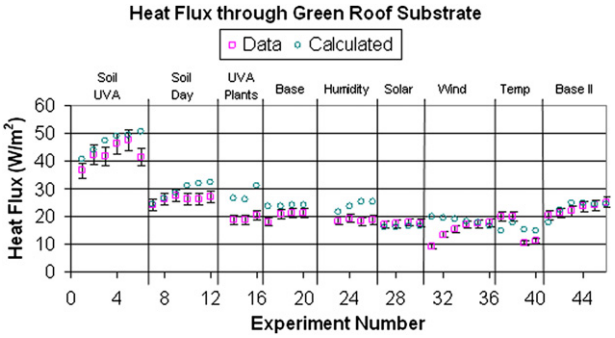

Fig. 7. Measured (squares) and calculated (circles) conduction heat fluxes.

3.3.3.2. Plant surface temperature. Fig. 9 shows measured (squares) and calculated (circles) plant surface temperatures. For this specific variable, there is no available data for the green roof samples without plants. Model predictions are generally good, with exception of the first couple of days. This trend has been consistent for all the heat transfer processes.

4. Discussion

A new green roof model is validated using quasi-steady state experimental data. To our best knowledge, this is the first study that performs this type of detailed validation approach. It is important to point out that none of the existing green roof models have performed this type of detailed model component validation. Consequently, it is not possible to assess how well they performed with respect to prediction of individual heat flux components. In this paper, the performance of the new green roof model during validation is analyzed in Table 4 based on normalized biases ([data-model]/data), root mean square errors (RMSE), and normalized root mean square errors (NRMSE). This validation showed that the model predicts most of the heat and mass transfer accurately, but it also underestimates maximal evapotranspiration rates. Due to the nature of the problem, the variables in the model are strongly inter-related. Fortunately results from the verification and validation showed very similar RMSE values. These are very encouraging results as it indicates that overall the model is able to obtain relative good accurate results.

Table 4 also shows that convection and evapotranspiration have similar RMSE but different NRMSE. In fact, evapotranspiration NRMSE for experiments without plants is very close to the convection NRMSE for experiments with plants. This is also

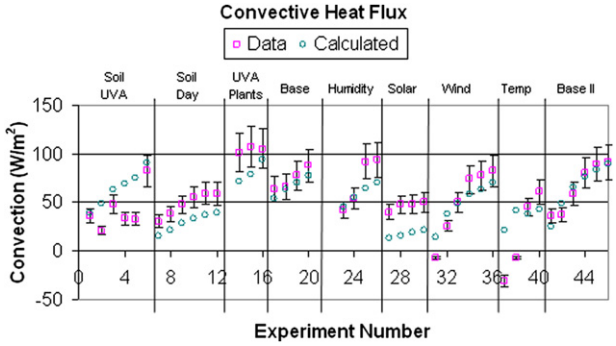

Fig. 6. Measured (squares) and calculated (circles) convective heat transfer.

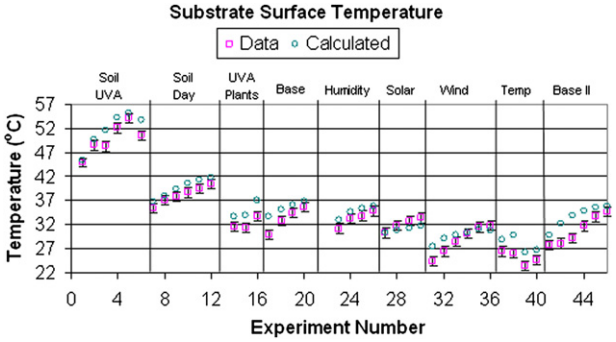

Fig. 8. Measured (squares) and calculated (circles) surface substrate temperatures.

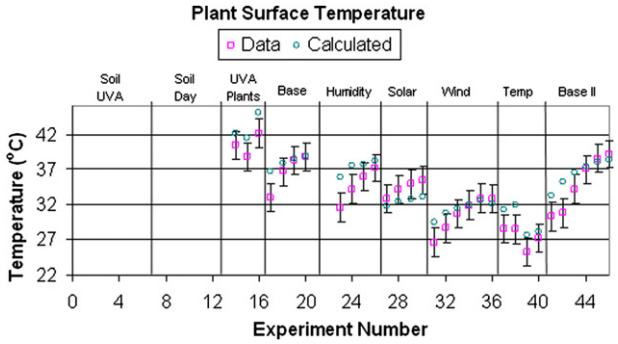

Fig. 9. Measured (squares) and calculated (circles) surface plant temperatures.

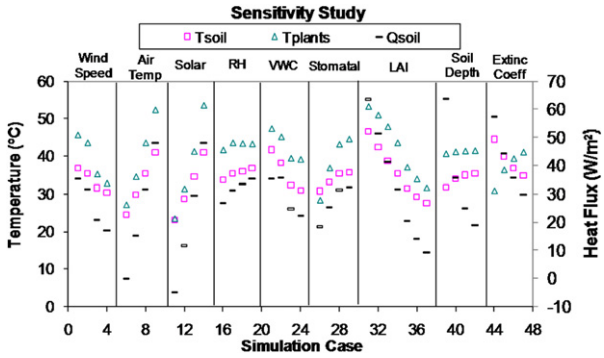

Fig. 10. Steady state analysis of substrate temperature (Tsoil), plant temperature (Tplants) and substrate heat flux (Qsoil) using validated model.

supported in Figs. 6 and 7. Moreover, Figs. 6 and 7 show that for two cases where the model predicts very closely evapotranspiration, it fails to predict correct convection heat transfer (Soil UVA and Solar experiments). RMSE of substrate and plant temperature is roughly 2 °C. From these two variables, plant temperature is specially difficult to measure, as leaves temperature is not homogeneous and detail infrared analysis in previous experimental work showed a standard deviation of 2 °C [53] from the central area of the green roof samples. Thus, the RMSE is between the expected ranges of temperature recorded by the infrared camera.

Table 4 also shows how well the model overall performed compared to experimental data. The results in Table 4 show differences in all variables that are outside of the experimental uncertainty except for surface temperatures [53,58]. Once validation for steady state conditions is done, it is now possible to conduct more in-depth analyses.

Fig. 10 shows how substrate temperature (T_{soil}), plant temperature (T_{plants}) and heat flux (Q_{soil}) through the substrate change when a specific environmental or green roof variable are changed under steady conditions. The top x-axis legend represents the variable that is being change from a minimum to a maximum value. Inputs for Fig. 10 are in the appendix, these hypothetical inputs are different than the experimental data used in the validation. Bottom substrate temperature was kept constant in all cases at 25 °C as well as the plant coverage that was kept at 0.98, green roof planter sample area equal to 1.3 m^2 and sky temperature equal to 15 °C.

From all environmental variables, solar energy is the variable with the strongest weight on the model results. In contrast, relative humidity had the least impact under the conditions tested. From all green roof design variables analyzed, LAI is the most significant factor reducing substrate temperature and heat flux through the substrate by increasing shading, convective heat transfer and evapotranspiration. Interestingly, water content in the substrate did not have one of the most significant impacts. However, changing substrate conditions from driest to the wettest conditions showed a 10 °C decrease in substrate temperature and 40% reduction in heat flux. This reduction was mainly due to an increase in evapotranspiration (from 8 to 230 W/m^2) despite an increase in substrate thermal conductivity (70%) and a decrease of 50% of substrate reflectivity. On the other hand, minimum stomatal values and extinction coefficients depend on plant selection. Values around 60 s/m (grass) produced evapotranspiration fluxes around 3-4 times higher than when minimum stomatal values for succulent plants were used. Higher evapotranspiration fluxes are beneficial, but provide less water control and/or might require irrigation in contrast with succulent plants that have higher minimum stomatal values. Finally, from the 4 different stomatal sub-functions (Equation (22)–(24)) Equation 24 (f_{VPD}) is the most sensitive environmental changes as vapor pressure differential depends on relative humidity, air temperature and plants/substrate temperature. Table A.1 also shows that aerodynamic resistance (r_a) play a very minor role and almost insignificant role in evapotranspiration as stomatal resistance values are about 8–20 times higher for the cases when minimum stomatal resistance of 700 s/m was used. Aerodynamic resistance plays a much important role when plants with lower resistance such as grass are used. However, it is important to accurately calculate aerodynamic resistance as it has a strong impact on convective heat transfer.

Further research on convective heat transfer for plants is recommended as well as a spectral reflectivity measurement of the substrate to improve the accuracy of the model. Table 5 shows the complete model components for the green roof completely cover by plants as well as the areas where most of the contributions of this study were done.

Table 4
Green roof model performance based on calculated normalized biases, root mean square errors (RMSE), and normalized root mean square errors (NRMSE) during validation.

	Green Roof Experiments without Plants			Green Roof Experiments with Plants		
	Normalized bias	RMSE	NRMSE	Normalized bias	RMSE	NRMSE
Evapotranspiration (W/m^2)	−0.24	21.4 W/m^2	0.29	0.04	23.0 W/m^2	0.20
Convection (W/m^2)	−0.16	17.0 W/m^2	0.20	0.55	18.0 W/m^2	0.30
Conduction (W/m^2)	−0.14	4.4 W/m^2	0.13	−0.19	4.0 W/m^2	0.21
Substrate Temperature (°C)	−0.06	1.8 °C	0.04	−0.038	2 .0 °C	0.07
Plant Temperature (°C)	N/A	N/A	N/A	−0.04	1.9 °C	0.08

Table 5
Summary of recommended equations for a green roof fully-covered by plants.

Heat Flux	Equation	New/Adopted/Modified Component
Energy Balance	$R_{sh,abs,plants} = Q_{film,plants} + Q_{IR,S,P}$	Modified
	$R_{sh,abs,substrate} = -Q_{IR,S,P} + Q_{s,s} + Q_{conduction} + Q_{IR,subs,cov,sky} + Q_E$	
Radiation	$R_{sh,abs,plants} = (1-\rho_{plants}-\tau_{plants,solar})(1+\tau_{plants}\rho_{substrate})R_{sh}$	Adopted
	$R_{sh,abs,substrate} = \tau_{plants,solar}(1-\alpha_{substrate})R_{sh}$	Adopted
	$Q_{IR,plants,sky} = (1-\tau_{plants,IR})\varepsilon_{plants}\sigma(T^4_{plants}-T^4_{sky})$	Adopted
	$Q_{IR,substrate,cov,sky} = (\tau_{plants,IR})\varepsilon_{substrate}\sigma(T^4_{plants}-T^4_{sky})$	Adopted
	$Q_{IR,S,P} = (1-\tau_{IR})\dfrac{\sigma\left(T^4_{plants}-T^4_{top,substrate}\right)}{\frac{1}{\varepsilon_{substrate}}+\frac{1}{\varepsilon_{plants}}-1}$	Adopted
Convection	$Q_{convection,plants} = 1.5\cdot LAI\cdot h_{conv}(T_{plants}-T_{air})$	Modified
	$N_u = \begin{cases} 3+1.25\times 0.025\mathrm{Re}^{0.8} & Gr < 0.068\mathrm{Re}^{2.2.} \quad \text{Forced Convection} \\ 2.7\left(\frac{Gr}{\mathrm{Re}^{2.2}}\right)^{1/3}\left(3\frac{15}{4}+\frac{15}{16}\times 0.0253\mathrm{Re}^{0.8}\right) & 0.068\mathrm{Re}^{2.2.} < Gr < 55.3\mathrm{Re}^{5/3} \quad \text{Mixed Convection} \\ 0.15Ra^{1/3} & 55.3\mathrm{Re}^{5/3} < Gr \quad \text{Natural Convection} \end{cases}$	Adopted
	$Q_{convection,substrate,cov} = h_{sub}(T_{substrate,top}-T_{air})$	New
	$h_{sub} = \dfrac{h_{por}\cdot h_{conv}}{h_{por}+h_{conv}}$	Adopted
	$h_{por} = \dfrac{k_{por}}{L}1.128Pe^{0.5}$	Adopted
	$Pe = 0.3V_{air}\dfrac{L}{\alpha_{por}}$	Modified
	$k_{por} = \phi\cdot k_{air}+(1-\phi)k_{plants}$	Adopted
Evapotranspiration	$Q_T = \mathrm{LAI}\dfrac{\rho C_p}{\gamma(r_s+r_a)}(e_{s,plants}-e_{air})$	Adopted
	$Q_E = \dfrac{\rho C_p}{\gamma(r_{soil}+r_a)}(e_{soil}-e_{air})$	Adopted
	$r_{substrate} = c_1 + c_2\left(\dfrac{\mathrm{VWC}}{\mathrm{VWC}_{sat}}\right)^{c_3}$	New
	$r_s = \dfrac{r_{stomatal,min}}{\mathrm{LAI}}\cdot f_{solar}\cdot f_{VPD}\cdot f_{vwc}\cdot f_{Temperature}$	Modified
	$f_{solar} = 1+e^{-0.034(R_{sh}-3.5)}$	Adopted
	$f_{VWC} = \begin{cases} 1 & \mathrm{VWC} > 0.7\mathrm{VWC}_{fc} \\ \dfrac{0.70\mathrm{VWC}_{fc}-\mathrm{VWC}_{wp}}{\mathrm{VWC}-\mathrm{VWC}_{wp}} & \mathrm{VWC}_{wp} < \mathrm{VWC} < 0.7\mathrm{VWC}_{fc} \\ 1000 & \mathrm{VWC}_{wp} > \mathrm{VWC} \end{cases}$	Modified
	$f_{VPD} = \dfrac{1}{1-0.41\ln(e_{s,plants}-e_a)}$	Adopted
	$f_{temperature} = \dfrac{1}{1-0.0016(35-(T_{plants}-273.15))^2}$	Modified
Conduction	$Q_{conduction} = k_{substrate}\dfrac{T_{top,substrate}-T_{bottom,substrate}}{L_{substrate}}$	Adopted
	$k_{substrate} = a_1 + a_2\times \mathrm{vwc}$	New

5. Conclusion

A new green roof model was proposed and validated using quasi-steady state experimental data. Since all heat fluxes in a green roof system are interconnected and dependent on each other, the model considers heat and mass transfer processes between the sky, plants, and substrate. Among the previous green roof, soil, and global climate research, our literature review found several different models to calculate: (1) substrate thermal conductivity, (2) the substrate and plants evapotranspiration, (3) radiative heat transfer between the plants and substrate, and (4) convection heat and mass transfer. Experimental data from the "Cold Plate" apparatus revealed that these models significantly overestimated or underestimated the substrate thermal conductivity, and evapotranspiration rates for green roof systems. For these reasons, a new substrate thermal conductivity equation was introduced as well as a new substrate resistance to soil evaporation based on laboratory experimental data collected in the "Cold Plate" apparatus. Furthermore, a new set of stomatal resistance functions were selected based on previous stomatal functions that best approximate the measured values. From the different radiative heat transfer models between the plants and substrate, evaluation and comparison of these models showed differences less than 10%. Thus, any of the plant-soil radiative models can be safely applied. Finally, the proposed model represents the plant layer as a porous media for convection heat and mass transfer purposes. This assumption decreases the number of energy balance required from 3 to only 2 (compared to previous models [42,44,46]) and simplifies subsequent equations needed in the modeling task without affecting the accuracy of the model. These new components improve the performance during the validation process.

To our knowledge, this is the first study that has performed this type of detailed approach for verification and validation of green roof model components. The validation shows that the model predicts most of the heat and mass transfer accurately, except that it underestimates maximum evapotranspiration rate, which can be linked to the overestimated stomatal resistance. The underestimation of evapotranspiration could also be attributed to the convective heat and mass transfer coefficient used, for flat plates with a multiplier of 1.5. Preliminary steady state analyzes shows that between all environmental factor analyzed solar radiation has the largest impact on heat fluxes, while relative humidity has the least. From the analyzed green roof parameters, LAI has the major effect in reducing heat flux through the roof in contrast with plant stomatal resistance and substrate thickness. These are preliminary values as no other components on a real roof have been evaluated, such as insulation, but highlight the importance of different variables.

Future research will validate the model in dynamic conditions as well as incorporate the mass balances in the model. This future study will be performed for a real building green roof based on the model created in the current study to assess the impact of a green roof fluxes on the building cooling loads.

Acknowledgment

We would like to thank Dr. Robert Berghage, Director of the Penn State Center for Green Roof Research, for his cooperation and assistance with the design and selection of green roof plants and substrate. This study was supported by the Center for Environmental Innovation in Roofing, Washington DC, USA, http://www.roofingcenter.org/, CONACYT (Consejo Nacional de Ciencia y Tecnologia), Mexico, http://www.conacyt.mx/, ASHRAE Graduate Student Grant-In-Aid and ASHRAE Technical Committee TC 4.4 Building Materials and Building Envelope Performance, http://tc44.ashraetcs.org/, the National Science Foundation (NSF) grant (CMMI-0900486) http://www.nsf.gov/, and in-kind contributions from Vaisala Inc and Kipp&Zonnen.

Appendix

Table A.1
Input and Output values from preliminar sensitivity study.

Name	Input/Analyzed Variables										Output											
	LAI	r_min (s/m)	Q_sun (W/m^2)	V (m/s)	Tair (°C)	RH	k_s long-wave	k_s short-Wave	L_{soil} (m)	VWC	$Q_{sun-abs\_soil}$ (W/m^2)	T_{soil} (°C)	T_{plants} (°C)	Q_{soil} (W/m^2)	Q_{ET} (W/m^2)	Q_{Conv} (W/m^2)	r_a (s/m)	r_s (s/m)	f_{VPD}	f_{VWC}	f_{solar}	f_{temp}
Wind	2	700	700	**0.1**	24.9	0.45	0.83	0.7	0.09	0.2	77.2	36.8	45.7	35.4	117.9	298.8	166	4324	8.1	1.3	1.0	1.2
Wind	2	700	700	**1**	24.9	0.45	0.83	0.7	0.09	0.2	108.4	35.5	43.6	31.7	145.9	273.7	163	2810	5.7	1.3	1.0	1.1
Wind	2	700	700	**2**	24.9	0.45	0.83	0.7	0.09	0.2	108.4	31.7	35.3	20.7	176.2	301.6	82	1083	2.5	1.3	1.0	1.0
Wind	2	700	700	**3**	24.9	0.45	0.83	0.7	0.09	0.2	108.4	30.5	32.9	17.1	172.2	320.6	60	922	2.1	1.3	1.0	1.0
Air Temp	2	700	700	1	**4.9**	0.45	0.83	0.7	0.09	0.2	108.4	24.5	27.2	0.0	151.1	363.8	157	928	1.9	1.3	1.0	1.1
Air Temp	2	700	700	1	**14.9**	0.45	0.83	0.7	0.09	0.2	108.4	29.8	34.6	15.2	173.3	301.8	162	1204	2.8	1.3	1.0	1.0
Air Temp	2	700	700	1	**24.9**	0.45	0.83	0.7	0.09	0.2	108.4	35.5	43.6	31.7	145.9	273.7	163	2809	5.7	1.3	1.0	1.1
Air Temp	2	700	700	1	**34.9**	0.45	0.83	0.7	0.09	0.2	108.4	41.1	52.4	47.9	73.1	286.3	142	170 278	202.3	1.3	1.0	1.9
Solar	2	700	**100**	1	24.9	0.45	0.83	0.7	0.09	0.2	15.5	23.2	23.5	−4.9	80.7	−24.2	143	686	1.2	1.3	1.0	1.3
Solar	2	700	**400**	1	24.9	0.45	0.83	0.7	0.09	0.2	62.0	28.7	31.4	11.7	145.2	109.2	143	848	1.9	1.3	1.0	1.0
Solar	2	700	**700**	1	24.9	0.45	0.83	0.7	0.09	0.2	108.4	34.6	41.3	29.2	161.0	275.5	143	1994	4.3	1.3	1.0	1.1
Solar	2	700	1000	1	24.9	0.45	0.83	0.7	0.09	0.2	154.9	41.0	53.6	48.0	112.7	483.2	142	19,464	20.0	1.3	1.0	2.2
RH	2	700	700	1	24.9	0.1	0.83	0.7	0.09	0.2	108.4	33.8	41.7	26.7	157.3	283.8	142	2921	6.2	1.3	1.0	1.1
RH	2	700	700	1	24.9	0.4	0.83	0.7	0.09	0.2	108.4	35.4	43.6	31.4	145.0	275.1	163	2983	6.0	1.3	1.0	1.1
RH	2	700	700	1	24.9	0.7	0.83	0.7	0.09	0.2	108.4	36.1	43.4	33.5	147.6	268.5	165	2160	4.4	1.3	1.0	1.1
RH	2	700	700	1	24.9	0.95	0.83	0.7	0.09	0.2	108.4	36.8	43.3	35.3	145.1	266.5	166	1745	3.6	1.3	1.0	1.1
VWC	2	700	700	1	24.9	0.45	0.83	0.7	0.09	0.05	96.3	41.8	47.4	35.4	8.8	350.5	154	42,452	12.2	7.5	1.0	1.3
VWC	2	700	700	1	24.9	0.45	0.83	0.7	0.09	0.15	104.9	38.2	45.2	35.8	84.5	306.9	159	5425	7.5	1.7	1.0	1.2
VWC	2	700	700	1	24.9	0.45	0.83	0.7	0.09	0.25	111.5	32.4	39.5	24.7	217.1	245.7	143	1283	3.5	1.0	1.0	1.0
VWC	2	700	700	1	24.9	0.45	0.83	0.7	0.09	0.3	114.1	31.0	39.2	22.1	235.5	239.5	143	1233	3.4	1.0	1.0	1.0
Stomatal	2	50	700	1	24.9	0.45	0.83	0.7	0.09	0.2	108.4	30.8	28.4	18.4	469.5	58.1	143	53	1.6	1.3	1.0	1.1
Stomatal	2	350	700	1	24.9	0.45	0.83	0.7	0.09	0.2	108.4	33.3	36.9	25.4	268.3	200.7	143	616	2.8	1.3	1.0	1.0
Stomatal	2	650	700	1	24.9	0.45	0.83	0.7	0.09	0.2	108.4	35.4	43.2	31.4	154.6	267.4	164	2468	5.4	1.3	1.0	1.1
Stomatal	2	950	700	1	24.9	0.45	0.83	0.7	0.09	0.2	108.4	35.8	44.6	32.5	118.5	293.4	161	4605	6.6	1.3	1.0	1.2
LAI	0.5	700	700	1	24.9	0.45	0.83	0.7	0.09	0.2	376.6	46.7	53.3	63.5	123.6	119.3	143	75,238	20.0	1.3	1.0	2.2
LAI	1	700	700	1	24.9	0.45	0.83	0.7	0.09	0.2	248.7	42.5	51.0	51.5	102.0	213.4	147	29,571	20.0	1.3	1.0	1.7
LAI	1.5	700	700	1	24.9	0.45	0.83	0.7	0.09	0.2	164.2	38.9	47.9	41.3	97.4	270.8	153	11,383	14.4	1.3	1.0	1.4
LAI	2	700	700	1	24.9	0.45	0.83	0.7	0.09	0.2	108.4	35.5	43.6	31.7	145.9	273.7	163	2809	5.7	1.3	1.0	1.1
LAI	2.5	700	700	1	24.9	0.45	0.83	0.7	0.09	0.2	71.6	31.6	37.1	20.5	227.8	255	143	1003	2.8	1.3	1.0	1.0
LAI	3	700	700	1	24.9	0.45	0.83	0.7	0.09	0.2	47.3	29.3	34.0	13.9	287.7	228.2	143	659	2.3	1.3	1.0	1.0
LAI	3.5	700	700	1	24.9	0.45	0.83	0.7	0.09	0.2	31.2	27.6	31.7	9.1	340.6	199.4	143	492	1.9	1.3	1.0	1.0
Soil Thick	2	700	700	1	24.9	0.45	0.83	0.7	0.03	0.2	108.4	31.9	40.7	63.6	153.9	265.3	143	1843	4.0	1.3	1.0	1.1
Soil Thick	2	700	700	1	24.9	0.45	0.83	0.7	0.07	0.2	108.4	34.1	41.2	35.7	159.7	273.5	143	1963	4.2	1.3	1.0	1.1
Soil Thick	2	700	700	1	24.9	0.45	0.83	0.7	0.11	0.2	108.4	35.0	41.4	24.7	162.1	276.8	143	2011	4.3	1.3	1.0	1.1
Soil Thick	2	700	700	1	24.9	0.45	0.83	0.7	0.15	0.2	108.4	35.4	41.5	18.9	163.3	278.5	143	2041	4.4	1.3	1.0	1.1
Ext Coeff	2	700	700	1	24.9	0.45	0.2	0.2	0.09	0.2	382.3	44.6	30.9	57.5	214.2	100.8	143	827	1.8	1.3	1.0	1.0
Ext Coeff	2	700	700	1	24.9	0.45	0.4	0.4	0.09	0.2	256.2	39.9	36.4	44.3	200.5	192.6	143	1182	2.7	1.3	1.0	1.0
Ext Coeff	2	700	700	1	24.9	0.45	0.6	0.6	0.09	0.2	171.8	36.9	39.4	35.7	180.1	243.4	143	1581	3.5	1.3	1.0	1.0
Ext Coeff	2	700	700	1	24.9	0.45	0.8	0.8	0.09	0.2	115.1	34.9	41.1	29.9	163.2	272.3	143	1945	4.2	1.3	1.0	1.1

Values in bold denote the input variable that is being modified and analyzed.

References

[1] Peck SW, Callaghan C. Greenbacks from green roofs: forging a new industry in Canada, prepared for: Canada mortgage and housing corporation. Environmental Adaptation Research Group, Environment Canada; 1999.
[2] Liu KKY, Baskaran BA. Green roof infrastructure – technology demonstration, monitoring and market expansion project. B1054.1. Institute for Research in Construction; 2004. p. 121.
[3] Snodgrass EC, Snodgrass LL. Snodgrass green roof plants: a resource and planting guide. Portland: Timber Press; 2006.
[4] Tanner S, Scholz-Barth K. Green Roofs, Federal Technology Alert DOE/EE-0298, Federal Energy Management Program (FEMP). U.S. Department of Energy; 2004.
[5] Johnston A. Annual green roof industry survey shows 24 per cent growth in North America. The Green Roof Infrastructure Monitor 2007;9(2):28.
[6] Peck SW. Green Roofs: Infrastructure for the 21st Century, Clean Air Partnership 1st Annual Urban Heat Island Summit, Toronto; 2002.
[7] Ross J. Radiative transfer in plant Communities. In: Monteith JL, editor. Vegetation and the Atmosphere. Principles, vol. 1. London: Academic Press; 1975. p. 13–55.
[8] Scurlock JM, Asner GP, Gower ST. Worldwide Historical estimates of leaf area index. 1932-2000 0RNL/TM-2001/268; 2001.
[9] Chen JM, Black TA. Defining leaf area index for non-flat leaves. Plant Cell Environ 1992;15:421–9.
[10] Nobel PS. Biophysical Plant Physiology and Ecology. San Francisco: W.H. Freeman and Company; 1983.
[11] Allen RG, Pereira LS, Raes D, Smith M. Crop evapotranspiration: Guidelines for computing crop requirements, Irrigation and Drainage Paper No. 56. Rome, Italy: Food and Agriculture Organization of the United Nations, <http://www.fao.org/docrep/X0490E/X0490E00.htm>; 1998.
[12] Hillel D. Environmental Soil Physics. San Diego: Academic Press; 1998.
[13] Bass B, Baskaran BA. Evaluating Rooftop and Vertical Gardens as an Adaptation Strategy for Urban Areas. Institute for Research in Construction, NRCC-46737; 2003. p. 110.
[14] Liu KKY, Baskaran BA. Thermal performance of green roofs through field evaluation, in: Proceedings for the First North American Green Roof Infrastructure Conference, Awards and Trade Show, Chicago, IL, May 5th 2003, pp. 1–10 (NRCC-46412).
[15] Denardo J. Green roof mitigation of stormwater and energy usage, M.S. thesis, Dept. of Horticulture, Pennsylvania State University, State College, PA, 2003.
[16] Wong N, Cheong H, Yan H, Soh J, Ong CL, Sia A. The effects of rooftop garden on energy consumption of a commercial building in Singapore. Energ Buildings 2003;35(4):353–64.
[17] Liu KKY, Minor J. Performance evaluation of and extensive green roof, third Annual International greening rooftops for sustainable Communities, in: Conference, Awards & Trade Show, Washington, DC, 2005.
[18] Sonne J. Evaluating green roof energy performance. ASHARE J February 2006; 48:59–61.
[19] VanWoert ND, Rowe DB, Andresen JA, Rugh CL, Xiao L. Watering regime and green roof substrate design affect sedum plant growth. HortScience 2005; 40(3):659–64.
[20] Rezaei F. Evapotranspiration rates from extensive green roof plant species. M.S. thesis, Agricultural and Biological Engineering, Pennsylvania State University, State College, PA, 2005.
[21] Berghage R, Jarrett A, Beattie D, Kelley K, Husain S, Rezai F, et al. Quantifying evaporation and transpiration water losses from green roofs and green roof media capacity for neutralizing acid rain. National Decentralized Water Resources Capacity Development Project; April 2007.
[22] Takebayashi H, Moriyama M. Surface heat budget on green roof and high reflection roof for mitigation of urban heat island. Build Environ 2000;42: 2971–9.
[23] Onmura S, Matsumoto M, Hokoi S. Study on evaporative cooling effect of roof lawn gardens. Energ Buildings 2001;33:653–66.
[24] Fang CF. Evaluating the thermal reduction effect of plant layers on rooftops. Energ Buildings 2008;40:1048–52.
[25] Bell H, Spolek G. Measured energy performance of green roofs, in: Seventh Annual International greening rooftops for sustainable Communities Conference, Atlanta, GA, June 2009.
[26] Tabares-Velasco PC, Srebric J. The role of plants in the reduction of heat flux through green roofs: laboratory experiments. ASHRAE Trans 2009;115(2): 793–802.
[27] Tabares-Velasco PC, Srebric J. Heat Fluxes and Water Management of a green and brown roof: laboratory experiments, Seventh Annual International greening rooftops for sustainable Communities Conference, Atlanta, GA, June 2009.
[28] Tabares-Velasco PC, Srebric J. Quantifying energy fluxes and water management of a green and brown roof: laboratory experiments. Living Architecture Monitor 2009;11(3):28–31.
[29] Liu KKY. Sustainable building envelope - garden roof system performance, 2004 RCI building Envelope Symposium. New Orleans, Louisiana, 2004 pp. 1–14 (NRCC-47354).
[30] Nayak JK, Srivastava A, Singh U, Sodha MS. The relative performance of different approaches to the passive cooling of roofs. Build Environ 1982;17(2): 145–1461.
[31] Eumorfopoulu E, Aravantinos D. The contribution of a planted roof to the thermal protection of buildings in Greece. Energ Buildings 1998;27:29–36.
[32] Niachou A, Papakonstantinou K, Santamouris M, Tsangrassoulis A, Mihalakakou G. Analysis of the green roof thermal properties and investigation of its energy performance. Energ Buildings 2001;33:719–29.
[33] Hilten R. An analysis of the energetics and stormwater mediation potential of greenroofs, M.S. thesis University of Georgia, Department of Biological and Agricultural Engineering, 2005.
[34] Saiz Alcazar S, Bass B. Energy performance of green roofs in a multi storey residential building in Madrid, in: Proceedings of the 3rd Annual Greening Rooftops for Sustainable Cities Conference, Washington, DC, 2005, pp. 14–27.
[35] Saiz Alcazar S. Greening the dwelling: a life cycle energy analysis of green roofs in residential buildings, M.S. Thesis Department of Civil Engineering, University of Toronto, Toronto, Ontario, 2004.
[36] Takakura T, Kitade S, Goto E. Cooling effect of green cover over a building. Energ Buildings 2000;31:1–6.
[37] Cappelli D, Cianfrini C, Corcione M. Effects of vegetation on roof shielding on indoor temperatures. Heat Technol 1998;16(2):85–90.
[38] Gaffin SR, Rosenzweig C, Parshall L, Beattie D, Berghage R, O'Keeffe G, Braman D. Energy balance modeling applied to a comparison of green and White roof cooling Efficiency, third Annual International greening rooftops for sustainable Communities, Conference, Awards & Trade Show, Washington, D.C., 2005, pp. 15–27.
[39] Gaffin SR, Rosenzweig C, Parshall L, Hillel D, Eichenbaum-Pikser J, Greenbaum A, Blake R, Beattie D, Berghage R. Quantifying evaporative cooling from green roofs and comparison to other land surfaces, in: Fourth Annual International Greening Rooftops for Sustainable Communities, Conference, Awards & Trade Show, Boston, MA, 2006, pp. 15–30.
[40] Howe C. Model for thermal analysis of green roof performance. Six Annual International greening rooftops for sustainable Communities, Conference, Awards & Trade Show, Baltimore, MD, 2008.
[41] Zhang JQ, Fang XP, Zhang HX, Yang W, Zhu CC. A heat balance model for partially vegetated surfaces. Infrared Phys Techn 1997;38:287–94.
[42] Alexandri E, Jones P. Developing a one-dimensional heat and mass transfer algorithm for describing the effect of green roofs on the built environment: comparison with experimental results. Build Environ 2007;42:2835–49.
[43] Lazzarin RM, Castelloti F, Busato F. Experimental measurements and numerical modeling of a green roof. Energ Buildings 2005;37:1260–7.
[44] Sailor DJ. A green roof model for building energy simulation programs. Energ Buildings 2008;40(8):1466–78.
[45] Pielke RA. Mesoscale Meteorological Modeling. New York: Academic Press; 2002.
[46] Palomo Del Barrio E. Analysis of the green roofs cooling potential in buildings. Energ Buildings 1998;27:179–93.
[47] Sailor DJ, Hutchinson D, Bokovoy L. Thermal property measurements for ecoroof soils common in the western U.S. Energ Buildings 2008;40:1246–51.
[48] Wang XA. An experimental study of mixed, forced and free convection heat transfer from a horizontal flat plate to air. Trans ASME 1982;104:139–44.
[49] Sun SF. Moisture and heat transport in a soil layer forced by atmospheric conditions. M.Sc. thesis, University of Connecticut, 1982. In: Camillo PJ, Gurney RJ. A resistance parameter for bare soil evaporation models. Soil Sci 141, 1986, pp. 95–105.
[50] Bussire F. Etude compare des evaporations de deux sols de Guadeloupe. D.A.A. ENSAM Montpellier, 1985, 21 pp + annexes. In: Tournebize R, Sinoquet H, Bussiere F. (Eds.), Modelling evapotranspiration partitioning in a Shrub/grass alley crop, Agricultural and Forest Metereology, vol. 81, (3–4), 1996, pp. 255–272.
[51] van de Griend A, Owe M. Bare soil surface resistance to evaporation by vapor diffusion under semiarid conditions. Water Resour Res 1994;30(2):181–8.
[52] Aluwihare S, Watanabe K. Measurement of evaporation on bare soil and estimating surface resistance. J Environ Eng 2003;129(12):1157–68.
[53] Tabares-Velasco PC, Srebric J. Experimental Quantification of heat and mass transfer process through vegetated roof samples in a new laboratory Setup, International Journal of heat and mass transfer, 2011, accepted.
[54] Passerat De Silans A, Bruckler L, Thony JL, Vauclin M. Numerical modeling of coupled heat and water flows during drying in a stratified bare soil comparison with field observations. J Hydrol 1989;105:109–38.
[55] Camillo PJ, Gurney RJ. A resistance parameter for bare soil evaporation models. Soil Sci 1986;141:95–105.
[56] Kondo J, Saigusa N. A parameterzation of evaporation from bare soi surfaces. J Appl Meteorol 1990;29:385–9.
[57] Olioso A, Chauki H, Wigueron J-P, Bergaoui K, Bertuzzi P, Chad A, et al. Estimation of energy fluxes from thermal infrared, spectral reflectances, microwave data and SVAT Modelling. Phys Chem Earth (B) 1999;24(7):829–36.
[58] Tabares-Velasco PC. Predictive Heat and Mass Transfer Model of plant-based roofing materials for Assessment of energy savings. Ph.D. Thesis, Dept. of Architectural Engineering, Pennsylvania State University, State College, PA, 2009.
[59] Ye Z, Pielke RA. Atmospheric parameterization of evaporation from nonplant-covered surfaces. J Appl Meteorol 1993;32:1248–58.
[60] Mahfouf JF, Noilhan J. Comparative study of various formulations of evaporation from bare soil using in situ data. J Appl Meteorol 1991;30:1354–65.
[61] Duffie JA, Beckman WA. Solar Engineering of Thermal Processes. New York: Wiley; 1991.

[62] Jones HG. Plants and Microclimate, Cambridge. Cambridge: University Press; 1992.
[63] Monteith JL, Unsworth MH. Principles of Environmental Physics. 3rd ed. London: Academic Press; 2008.
[64] Perino M, Serra V, Filippi M. Monitoraggio del comportamento termico di un tetto verde: primi risultati sperimentali, Congresso nazionale ATI 2003, Padova, Italy, 2003 pp. 1863–1872.
[65] Gates DM, Keegan HJ, Schleter JC, Weidner VR. Spectral properties of plants. Appl Opt 1965;4(1):11–20.
[66] Gates DM. Biophysical Ecology. New York: Springer-Verlag; 1980.
[67] Norman JM. Scaling processes between leaf and canopy levels. In: Ehleringer JR, Field CB, editors. Scaling physiological processes: Leaf to globe. California: Academic Press INC; 1993.
[68] Incropera FP, Dewitt DP. Fundamentals of Heat and Mass Transfer. New York: John Wiley & Sons; 2002.
[69] Schuepp PH. Tansley review No. 59 leaf boundary layer. New Phytol 1993; 125(3):477–507.
[70] Bejan A. Convection heat transfer. 3rd ed. Hoboken, New Jersey: John Wiley and Sons; 2004.
[71] Deardorff JW. Efficient prediction of ground surface temperature and moisture, with inclusion of a layer of vegetation. J Geophys Res 1978;83:1889–903.
[72] Hayes RL. The thermal conductivity of leaves. Planta (Ber); 1975:125–287.
[73] Jarvis PG. The interpretation of the variations in leaf water potential and stomatal conductance found in canopies in the field. Philos Trans Roy Soc London 1976;273B:593–610.
[74] Dickinson RE. Modeling evapotranspiration for three-dimensional global climate models. In: Hanson JE, Takahashi T, editors. Climate processes and climate sensitivity, vol. 29. Amer. Geophys. Union, Geophys. Monogr.; 1984. p. 58–72.
[75] Stahghellini C. Transpiration of greenhouse crops. Ph.D. Dissertation, Agricultural University, Wageningen, 1987. In: Palomo Del Barrio E. Analysis of the Green Roofs Cooling Potential in Buildings, Energy and Buildings 27, 1998, pp. 179–193.
[76] Stewart JB. Modeling surface conductance of pine forest. Agr Forest Meteorol 1988;43:19–35.
[77] Avissar R, Pielke RA. The impact of plant stomatal control on mesoscale atmospheric circulations. Agr Forest Meteorol 1991;54:353–72.
[78] Jacquemin B, Noilhan J. Sensitivity study and validation of a land surface parameterization using the Hapex-Mobilhy data set. Bound-Lay Meteorol 1990;52:93–134.
[79] Dolman AJ. A multiple-Source land-surface energy balance model for use in general circulation models. Agr Forest Meteorol 1993;65:21–45.
[80] Oren R, Sperry JS, Katul GG, Pataki DE, Ewers BE, Phillips N, et al. Survey and synthesis of intra- and interspecific variation in stomatal sensitivity to vapour pressure deficit. Plant Cell Environ 1999;22:1515–26.
[81] Ogle K, Reynolds JF. Desert dogma revisited: coupling of stomatal conductance and photosynthesis in the desert shrub, Larrea tridentate. Plant Cell Environ 2002;25:909–21.
[82] van de Hurk BJJM, Viterbo P, Beljaars ACM, Betts AK. Offline validation of the ERA40 surface scheme, Internal Report from ECMWF 295, 2002.
[83] Ronda RJ, De Bruin HAR, Holtslag AAM. Representation of the canopy conductance in modeling the surface energy budget for low vegetation. J Appl Meteorol 2001;40(8):1431–44.
[84] Noihlan J, Planton S. A Simple parameterization of land surface Processed for meteorological models. Mon Weather Rev 1989;117(3):536–49.
[85] Willmerm C, Fricket M. Stomata. 2nd ed. Chapman & Hall; 1996.
[86] ASHRAE.. ASHRAE handbook fundamentals. Atlanta: ASHRAE; 2005.
[87] AIAA. Guide for the verification and validation of computational fluid dynamics simulations. AIAA G-077-1998; 1998.
[88] ERCOFTAC. The ERCOFTAC best practice guidelines for industrial computational fluid dynamics. In: Casey M, Wintergerste T, editors. Ver. 1.0, ERCOFTAC special interest group on quality and trust in industrial CFD. CH-1015, Lausanne, Switzerland: ERCOFTAC Coordination Centre STI-LMF-EPFL. p. 95, <http://www.personal.psu.edu/jhm/ME540/lectures/VandV/VandVdefinitions.html>; 2000.

Nomenclature

a_1: substrate thermal conductivity coefficient, 0.17 for an expanded clay based substrate
a_2: substrate thermal conductivity coefficient, 0.37 for an expanded clay based substrate
c_1: substrate evaporative resistance coefficient, 0.0 for an expanded clay based substrate
c_2: substrate evaporative resistance coefficient, 34.5 for an expanded clay based substrate
c_3: substrate evaporative resistance coefficient, -3.3 for an expanded clay based substrate
Cp: specific heat of air, J/kg K
e_{air}: vapor pressure of the air, kPa
e_{soil}: vapor pressure at the soil/substrate surface, kPa
$e_{s,plants}$: vapor pressure of the air in contact with plants, kPa
ET: evapotranspiration, or latent heat flux by convection, W/m^2
f_{solar}: empirical multiplicative functions for solar irradiance role on stomatal aperture
$f_{temperature}$: empirical multiplicative functions for plant temperature role on stomatal aperture
f_{VPD}: empirical multiplicative functions for vapor pressure deficit (VPD) role on stomatal aperture
f_{VWC}: Empirical multiplicative functions for Substrate Volumetric Water Content (VWC) role on stomatal aperture
Gr: Grashof number
h_{conv}: convective heat transfer for plant layer, W/m^2 K
h_{por}: convective heat transfer for porous media (plants), W/m^2 K
h_{sub}: total convective heat transfer for green roof substrate covered by plants, W/m^2·K
i_{fg}: enthalpy of vaporization of water, J/kg
k_{plants}: thermal conductivity of leaves, 0.50 W/m·K (Hays 1975)
k_{por}: thermal conductivity of plant-air layer, W/m·K
k_{air}: thermal conductivity of air layer, W/m·K
k_s: extinction coefficient,
$L_{substrate}$: substrate depth, m
L: characteristic length of green roof, m
LAI: leaf area index [(leaf area)/ (soil surface)]
M: metabolic storage (photosynthesis and respiration), W/m^2
Nu: Nusselt number
Nu_{por}: Nusselt number for porous media
P: atmospheric pressure, kPa
Pe: Péclet number
$Q_{convection,plants}$: sensible heat flux between plants and surround air by convection, W/m^2
$Q_{convection,substrate,cov}$: sensible heat flux between substrate underneath plants and surround air by convection, W/m^2
$Q_{S,S}$: sensible heat flux between green roof substrate and surround air by convection, W/m^2
Q_E: soil evaporative flux, W/m^2
$Q_{IR,,subs,cov,sky}$: thermal radiation or radiative heat exchange between substrate and sky, W/m^2
$Q_{IR,plants,sky}$: thermal radiation or radiative heat exchange between plants and sky, W/m^2
$Q_{IR,S,P}$: radiative heat transfer between the plant layer and the top substrate layer, W/m^2
$Q_{conduction}$: conductive heat flux through green roof substrate, W/m^2
Q_T: plants transpiration flux, W/m^2
$Q_{sensible}$: sensible heat flux by convection, W/m^2
$Q_{conduction}$: conductive heat flux trough roof, W/m^2
r_a: aerodynamic resistance to mass transfer, s/m
Re: Reynolds number
r_s: stomatal resistance to mass transfer
$r_{stomatal,min}$: minimum stomatal resistance to mass transfer
R_n: net radiation
R_{sh}: solar or short-wave radiation on the surface
$R_{sh,abs}$: absorbed solar radiation by the green roof substrate
$R_{sh,abs,plants}$: absorbed short-wave or solar radiation by the plants
$R_{sh,abs,substrate}$: absorbed solar radiation by substrate underneath the plants
$r_{substrate}$: substrate surface resistance to mass transfer
$S_{thermal}$: thermal storage for substrate, plants, W/m^2
T_{plants}: plants' average temperature, K
T_{sky}: sky temperature, K
$T_{top,substrate}$: substrate outer layer temperature, K
$T_{bottom,substrate}$: substrate inner layer temperature, K
V_{air}: wind speed, m/s
VWC: substrate volumetric water content
VWC_{sat}: substrate volumetric water content at saturated conditions
VWC_{fc}: substrate volumetric water content at field conditions
VWC_{wp}: substrate volumetric water content at wilting point
γ: psychrometric constant $=C_pP/0.622i_{fg}$
ϕ: porosity of plant layer
ρ_{leaf}: albedo or reflectivity of the leafs
$\rho_{substrate}$: albedo or reflectivity of the substrate
σ: Stefan-Boltzmann constant, 5.64×10^{-8} W/m^2 K^4
σ_f: the plant coverage rate of a green roof
τ_d: canopy transmittance of diffuse radiation
$\tau_{plants,IR}$: long-wave transmittance of a canopy
$\tau_{plants,solar}$: shortwave transmittance of a canopy